University of Wollongong
Research Online

Faculty of Engineering and Information Sciences - Papers: Part A

Faculty of Engineering and Information Sciences

2015

Improved method for estimation of multiple parameters in self-mixing interferometry

Yan Gao
University of Wollongong, yg904@uowmail.edu.au

Yanguang Yu
University of Wollongong, yanguang@uow.edu.au

Jiangtao Xi
University of Wollongong, jiangtao@uow.edu.au

Qinghua Guo
University of Wollongong, qguo@uow.edu.au

Jun Tong
University of Wollongong, jtong@uow.edu.au

See next page for additional authors

Improved method for estimation of multiple parameters in self-mixing interferometry

Abstract

There are two categories of applications for self-mixing interference (SMI)-based sensing: (1) estimation of parameters associated with a semiconductor laser (SL) and (2) measurement of the metrological quantities of the external target. To achieve high resolution sensing, each category of applications requires knowledge from the other. This paper proposes an improved method that can simultaneously measure the parameters of an SL and the target movement in arbitrary form. Starting with the existing SMI model, we derive a new matrix equation for the measurement. The measurement matrix is built by employing all the available data samples obtained from an SMI signal. The total least squares estimation approach is used to estimate the parameters. The proposed method is verified by both simulations and experiments. (C) 2015 Optical Society of America

Authors

Yan Gao, Yanguang Yu, Jiangtao Xi, Qinghua Guo, Jun Tong, and Sheng Tong

An improved method for estimation of multiple parameters in a self-mixing interferometry

Yan Gao, Yanguang Yu*, Jiangtao Xi, Qinghua Guo, Jun Tong and Sheng Tong

School of Electrical, Computer and Telecommunications Engineering, University of Wollongong— Northfields Ave, Wollongong, NSW, 2522, Australia
Corresponding author: yanguang@uow.edu.au

There are two categories of applications for self-mixing interference (SMI) based sensing: 1) estimation of parameters associated with a semiconductor laser (SL) and 2) measurement of the metrological quantities of the external target. To achieve high resolution sensing, each category of applications requires the knowledge from the other. This paper proposes an improved method which can simultaneously measure the parameters of an SL and the target movement in arbitrary form. Starting with the existing SMI model, we derive a new matrix equation for the measurement. The measurement matrix is built by employing all the available data samples obtained from an SMI signal. The Total Least Square estimation approach is used to estimate the parameters. The proposed method is verified by both simulations and experiments. © 2014 Optical Society of America

1.Introduction

In recent years, much study has been done into the use of self-mixing interference (SMI) as a promising technique for non-contact sensing and its instrumentation [1-20]. A basic SMI system is illustrated in Fig. 1. It consists of three parts: a semiconductors laser (SL) and its controllers as the light source, a moving target to be measured forming the external cavity and a laser intensity detection block. The self-mixing effect occurs when some of the light emitted by the SL is backscattered or reflected by the external target and re-enters the laser cavity, leading to a modulated lasing field in both amplitude and phase. The modulated laser intensity detected by a monitor photodiode (PD) which is packaged at the rear facet of the SL, called an SMI signal, carries the information about both the target movement and the parameters associated with the SL.
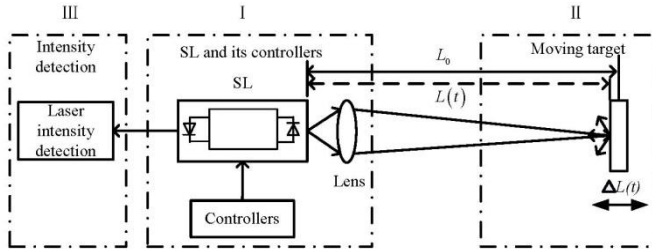

Fig. 1. SMI system

A widely accepted mathematical model for describing the SMI can be written as [3-5, 7, 8, 21, 22]:

$$\phi_0(t) = 4\pi L(t)/\lambda_0 \tag{1}$$

$$\phi_0(t) = \phi_F(t) + C \cdot \sin\left[\phi_F(t) + \arctan(\alpha)\right] \tag{2}$$

$$p(t) = p_0[1 + m \cdot g(t)] \tag{3}$$

$$g(t) = \cos\left(\phi_F(t)\right) \tag{4}$$

where t is the time index. Eq. (1) describes the connection between the laser phase and the external cavity length where $\phi_0(t)$ and λ_0 are the laser phase and the emitting wavelength of the free running laser, and $L(t)$ is the instantaneous external cavity length (shown in Fig. 1). Eq. (2) is the SMI phase condition equation which was developed from the Lang-Kobayashi (L-K) theory [23]. It describes the laser phase changes with the existence of optical feedback where $\phi_F(t)$ is the laser phase with the external feedback. C and α, are the optical feedback level factor and the linewidth enhancement factor, respectively, which describe the operating characteristics of the SMI system. Eq. (3) shows the SL emitting power intensity, where $p(t)$ and p_0 are laser intensities with and without the external cavity optical feedback, respectively. It can be seen that the laser intensity of a free running SL is modulated by a factor of $m \cdot g(t)$ when there is an external cavity, where m is the modulation index (typically $m \approx 10^{-3}$). $g(t)$, described in Eq. (4), reveals the influence of the external cavity to the laser intensity through $\phi_F(t)$. Since $p(t)$ can be detected by a PD enclosed in the package of the semiconductor laser, the $g(t)$ can be obtained through data processing on $p(t)$ via $g(t) = \left[p(t) - p_0\right]/mp_0$. Thus physical quantities associated with the system parameters (e.g. the linewidth enhancement factor and the optical feedback level

factor) and the external cavity (e.g. displacement, velocity or movement, etc.) can be retrieved from $g(t)$ based on Eqs.(1)-(4).

One category of the applications using the SMI system is to measure the parameters associated with the SL, e.g. linewidth enhancement factor and the optical feedback level factor [2, 5, 7, 9-11, 24]. The linewidth enhancement factor, also called the alpha factor ($\alpha - factor$), is one of the fundamental parameters in SLs as it characterizes the SL linewidth, the chirp, the injection lock range and the response to optical feedback. Measurement of α has been extensively studied using various methods [25, 26]. The optical feedback level factor, denoted as C, categorizes the operational modes of an SMI system according to the optical feedback levels, namely, the weak feedback regime($0 < C < 1$), the moderate feedback regime: ($1 < C < 4.6$) and the strong feedback regime ($C > 4.6$). In recent years, a number of SMI-based approaches have been proposed for measuring C and α [2, 5, 7, 9-11, 24]. However, these methods have the following limitations: 1) they require an SMI system to operate in a certain feedback range, e.g. the methods in [5, 7, 9] are valid for weak feedback regimes ($0 < C < 1$) and the method in [2] is only for a moderate regime $1 < C < 3$; 2) they require knowledge of the movement of the external cavity [5, 7, 9] and the movement must be in a simple harmonic way; 3) they require complex signal processing techniques such as phase unwrapping (PUM) [10] and data-to-model fitting with genetic algorithms [5, 7, 9]. These requirements make system implementation difficult.

Another category of the applications is on the measurement of the target movement. The dynamic range of measurement displacement is limited by the laser diode coherence length [1,12,13,15]. In general, the resolution of SMI-based measurement using the fringe counting method is half-wavelength [13]. The resolution can be greatly improved by sophisticated signal pre-processing [27, 28], fringe sub-division [14-16] and SMI model-based reconstruction [3-5, 10, 17-19]. However, all proposed methods for measuring the target movement can only be used within a certain range of C. All the methods based on fringe sub-division are only valid in a moderate feedback regime where $1 < C < 4.6$. Ignoring the influence of parameters C and α on fringe-shape or fringe-loss in strong feedback regimes will lead to detection errors. Existing model-based methods also suffer from a restriction in the C range, e.g., the method in [5] only works in a weak feedback regime where $0 < C < 1$ and the method in [3, 4] is only valid

when $1 < C < 4.6$. In addition, the accurate values for α and C are required by methods [3, 10, 17, 18], and this is not always possible in practice. The accuracy associated with the method using the Fourier transform method [19] is also limited due to the neglect of the second and higher order of the Fourier Transform in estimation.

In summary, the SMI based applications in one of above two categories requires the knowledge from the other, e.g. the estimation of the parameters associated with the SL requires the knowledge of the target movements while the accurate measurement of the target movements needs to know the knowledge on C and α. For solving this problem, [29] presented a method to measure C, α and the target movement simultaneously. However, the method in [29] only works when the target is subject to a periodic movement. The purpose of this paper is to present a new approach which is able to simultaneously retrieve SL related parameters and the target movement in arbitrary form, thus lifting all the restrictions in existing methods.

2.Proposed method

Let us use Fig. 1 to describe the proposed method. The length of the external cavity is expressed by $L(t) = L_0 + \Delta L(t)$, where L_0 is the length at the equilibrium point of the moving target and $\Delta L(t)$ is the instantaneous displacement of the target relative to the equilibrium point. The light phase $\phi_0(t)$ is related to $L(t)$ by $\phi_0(t) = \frac{4\pi}{\lambda_0}L_0 + \frac{4\pi}{\lambda_0}\Delta L(t)$. Supposing the target is moving in an arbitrary form, $\phi_0(t)$ can be expressed by a polynomial as below:

$$\phi_0(t) = \sum_{n=0}^{N} c_n t^n \tag{5}$$

where N is the order of the polynomial, $c_0 = \frac{4\pi}{\lambda_0}L_0$ and c_n $(n \neq 0)$ are the zero order and other higher order coefficients of the polynomial, respectively. Taking derivative of Eqs. (2), (4) and (5) with respect to t, after substituting and re-arrangement, we have:

$$\frac{dg(t)}{dt} = -\frac{dg(t)}{dt}g(t)u_1 + \frac{dg(t)}{dt}\sqrt{1-g^2(t)}u_2 - \sqrt{1-g^2(t)}\sum_{n=1}^{N} c_n n t^{n-1} \quad,(\text{when } \frac{dg(t)}{dt} < 0) \tag{6a}$$

and

$$\frac{dg(t)}{dt} = -\frac{dg(t)}{dt}g(t)u_1 - \frac{dg(t)}{dt}\sqrt{1-g^2(t)}u_2 + \sqrt{1-g^2(t)}\sum_{n=1}^{N} c_n n t^{n-1} \quad,(\text{when } \frac{dg(t)}{dt} > 0) \tag{6b}$$

where $u_1 = C\cos(\arctan(\alpha))$ and $u_2 = C\sin(\arctan(\alpha))$ \hfill (7)

In Eq. (6), $g(t)$ is the observed SMI signal from an SMI system and $dg(t)/dt$ is the derivative of $g(t)$. It can be seen Eq.

(6a)/6(b) is a linear equation with u_1, u_2 and c_n as variables, in total $N+2$ variables. Generally, $N+2$ variables can be solved by establishing $N+2$ independent equations using the obtained

data samples from $g(t)$ and its corresponding $dg(t)/dt$. In order to improve the accuracy of the solutions to the variables, we propose to use all data samples from the observed signal, that is, we will employ much more than $N+2$ samples. Suppose that we have M_1 data samples satisfying Eq 6(a) and M_2 samples satisfying Eq. 6 (b). By introducing $A(t)=(dg(t)/dt)g(t)$, $B(t)=(dg(t)/dt)\sqrt{1-g^2(t)}$, $C_n(t)=n\sqrt{1-g^2(t)}t^{n-1}$, where $n=1:N$, we can build a matrix Eq. (8) as below:

$$\mathbf{G} = \mathbf{H}\boldsymbol{\theta} \tag{8}$$

where

$$\boldsymbol{\theta} = [u_1, u_2, c_1, \cdots c_N]^T \tag{9}$$

$$\mathbf{G} = \left[\frac{dg(t_1)}{dt}, \frac{dg(t_2)}{dt}, \cdots \frac{dg(t_{M_1})}{dt}, \frac{dg(t'_1)}{dt}, \frac{dg(t'_2)}{dt}, \cdots, \frac{dg(t'_{M_2})}{dt}\right]^T \tag{10}$$

$$\mathbf{H} = \begin{bmatrix}
-A_1(t_1) & B_2(t_1) & -C_1(t_1) & -C_2(t_1) & \cdots & -C_N(t_1) \\
-A_1(t_2) & B_2(t_2) & -C_1(t_2) & -C_2(t_2) & \cdots & -C_N(t_2) \\
\vdots & \vdots & \vdots & \vdots & \ddots & \vdots \\
-A_1(t_{M_1}) & B_2(t_{M_1}) & -C_1(t_{M_1}) & -C_2(t_{M_1}) & \cdots & -C_N(t_{M_1}) \\
-A_1(t'_1) & -B_2(t'_1) & C_1(t'_1) & C_2(t'_1) & \cdots & C_N(t'_1) \\
-A_1(t'_2) & -B_2(t'_2) & C_1(t'_2) & C_2(t'_2) & \cdots & C_N(t'_2) \\
\vdots & \vdots & \vdots & \vdots & \ddots & \vdots \\
-A_1(t'_{M_2}) & -B_2(t'_{M_2}) & C_1(t'_{M_2}) & C_2(t'_{M_2}) & \cdots & C_N(t'_{M_2})
\end{bmatrix}_{(M_1+M_2)\times(N+2)} \tag{11}$$

Since Eq. (10) and Eq. (11) are built by experimental data samples, we use $\hat{\mathbf{H}}$ and $\hat{\mathbf{G}}$ to denote $\mathbf{H}$ and $\mathbf{G}$ in practice. By introducing perturbations on both sides of Eq. (8), denoted as $\mathbf{E}$ and $\mathbf{r}$, the practical estimation model should be expressed by:

$$\hat{\mathbf{G}} + \mathbf{r} = (\hat{\mathbf{H}} + \mathbf{E})\boldsymbol{\theta} \tag{12}$$

According to the Total Least Square (TLS) estimation approach [30, 31], the optimal solutions of $\hat{\boldsymbol{\theta}}_{opt}$ can be found by

$$\underset{\mathbf{E},\mathbf{r}}{\text{minimize}} \quad \|(\mathbf{E}\ \ \mathbf{r})\|_F \tag{13}$$

which subjects to the constraint $\hat{\mathbf{G}} + \mathbf{r} = (\hat{\mathbf{H}} + \mathbf{E})\boldsymbol{\theta}$.

We have the optimal $\hat{\boldsymbol{\theta}}_{opt}$ as below:

$$\hat{\boldsymbol{\theta}}_{opt} = (\hat{\mathbf{H}}^T\hat{\mathbf{H}} - \sigma^2\mathbf{I})^{-1}\hat{\mathbf{H}}^T\hat{\mathbf{G}} \tag{14}$$

where σ is the smallest singular value of matrix $\mathbf{S} = [\hat{\mathbf{H}}\ \ \hat{\mathbf{G}}]$.
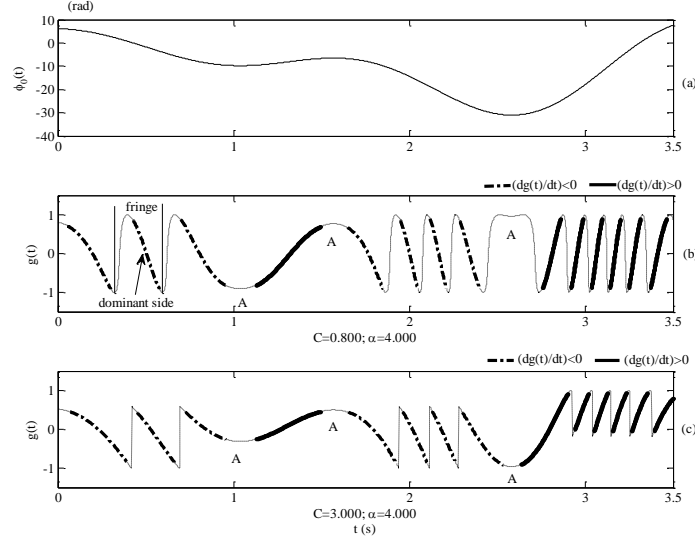

Fig. 2. Illustration for samples division rules. (a) laser phase $\phi_0(t)$ corresponds to an arbitrary displacement $\Delta L(t)$; (b) simulated SMI signal in weak feedback regime $C/\alpha = 0.800/4.000$; (c) simulated SMI signal in moderate feedback regime $C/\alpha = 3.000/4.000$.

Generally speaking, the more samples we use in the TLS estimation, the better result we can obtain. Unlike the method in [29], we will use all available data samples instead of the samples chosen in [29]. This means that the correct sample areas must be determined in $g(t)$ and its corresponding derivative version $dg(t)/dt$. The target movement is depicted in Fig. 2(a) and its corresponding SMI signals in weak and moderate feedback regimes are plotted in Fig. 2 (b) and (c), respectively. The

divisions for the case using Eq. (6a) and the case using Eq. (6b) are made based on the following:

- The data samples are only taken from the dominant side (indicated by thick line) within each fringe and divided into two groups according to the sign of $dg(t)/dt$: the dash-dotted line indicates that

$(dg(t)/dt) < 0$ and the solid line indicates that $(dg(t)/dt) > 0$;

- The data samples near the peak and near the bottom of each fringe which violate the condition that $dg(t)/dt \neq 0$, as shown by the dotted lines, are excluded;

- The area corresponding to the point at which the target changes its direction, shown as 'A' areas in Fig. 2(b) and 2(c), is avoided.

Based on above criteria, the data samples can be selected to form $\hat{\mathbf{H}}$ and $\hat{\mathbf{G}}$. And then the optimal parameters $\hat{\boldsymbol{\theta}}_{opt}$ can be obtained using Eq. (14). And then parameters C and α can be calculated using Eq. (7) by $C = \sqrt{u_1^2 + u_2^2}$ and $\alpha = u_2/u_1$, and the target trajectory of $\phi_0(t)$ can be calculated by Eq. (5) using the estimated $[c_1, c_2, \cdots, c_N]^T$.

3.Verification

A.Simulation verification

As an example, in order to verify the proposed method, we first apply the proposed approach on the simulation data generated by the SMI model described in Eqs. (1)-(4). Suppose that a target with an arbitrary form of the movement is introduced:

$$\phi_0(t) = 6.25t\cos(t) + 2.5\sin\left[(0.005t)^2\right] - 3t\cos(3.5t) \quad (15)$$
$$t \in [0, \ 10 \ s]$$

For the SMI model, we set two pairs of C and α with C/α as 0.800/4.000 and 3.000/4.000, respectively. Then $\phi_0(t)$ and the corresponding SMI signal can be generated and shown in Fig. 3 (a)/(b) and Fig. 3 (e)/(f). The reconstructed target movement
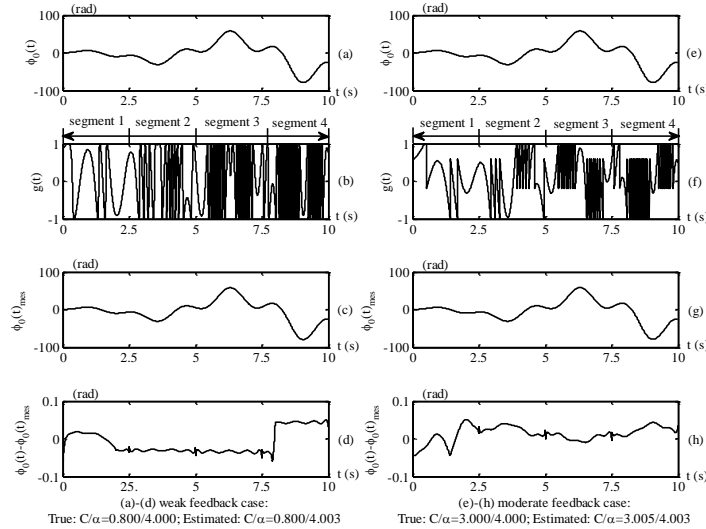
(denoted by $\phi_0(t)_{mes}$) using the proposed method and the error associated with the estimation are shown in Fig. 3(c)/(d) and Fig. 3(g)/(h) for the two cases. In general, for a segment of SMI signal with M' data samples selected, the computational burden in terms of multiplications for TLS estimation using an $N-th$ order polynomial is $O\left(M'(N+2)^2\right)$. The more complex the movement waveform, the higher the order of the polynomial (N) required, and the larger the number of data samples (M') are required to form the $\mathbf{H}$. In order to reduce N and M' , we can divide the SMI signal into short and simple segments, which are processed on a segment-by-segment basis using the above-described method. The computer simulations were carried out according to the following:

Step 1: a piece of $g(t)$ was segmented into segments, and for each of the segments the following steps were carried out:

Step 2: data samples within each segment was taken according to the division rules shown in Fig. 2;

Step 3: proper data samples were taken to build $\hat{\mathbf{G}}$ and $\hat{\mathbf{H}}$ by Eq. (10) and Eq. (11), respectively;

Step 4: Eq. (14) was solved in order to yield the parameters u_1, u_2 and all polynomial coefficients c_n ;

Step 5: Eq. (7) was used to obtain C and α , and the target movement $\phi_0(t)$ corresponding to the current segment $g(t)$ was reconstructed using the estimated parameters using Eq. (5);

Step 6: Step 2-5 were repeated with each segment;

Step 7: all reconstructed $\phi_0(t)$ were gathered together sequentially and the average of C and the average of α can be obtained.

Fig. 3. Reconstruction results for arbitrary movement. (a)-(d) reconstruction results for a weak feedback regime with true values: $C/\alpha = 0.800/4.000$; (e)-(h) reconstruction results for a moderate feedback regime with true values: $C/\alpha = 3.000/4.000$.

For the example of the target trajectory $\phi_0(t)$ shown in Fig. 3, its corresponding SMI signals in weak feedback and moderate feedback regimes are depicted in Fig. 3(b) and 3(f), respectively

with the sampling rate of 100 kHz. Thus there are 1×10^6 data samples in total for each case. If we apply the TLS estimation on the whole piece of the SMI at once, N is required to be 35

according to the simulation. Hence the overall maximum computing burden is $O\left(\left(1\times10^6\right)\times37^2\right)$, which is obviously very heavy. For this reason, we divided it into four segments with the same signal length to do the TLS estimation. Both the order of the polynomial and the number of data samples can be greatly reduced. There are 2.5×10^5 data samples in each segment, and a $10-th$ order polynomial is sufficient to fit each segment of $\phi_0(t)$ which reduces the maximum computational complexity to $O\left(\left(2.5\times10^5\right)\times12^2\right)$. The variation range of $\phi_0(t)$ in Fig. 3 is 137.189 rad which corresponds to $8.734\,\mu m$ of the displacement range if the wavelength of the laser is $0.8\,\mu m$. It can be seen from Fig.3 that for both cases, the reconstructed results $\phi_0(t)_{mes}$ are very close to $\phi_0(t)$, with the maximum absolute deviation less than $0.0022\,\mu m$ (0.0351 rad) and $0.0020\,\mu m$ (0.0317 rad) respectively, and the relative deviations are 0.03% and 0.02% respectively. Regarding to the estimation of two parameters, C and α, for the case of $C/\alpha=0.800/4.000$, we obtained $\tilde{C}/\tilde{\alpha}=0.800/4.003$ with accuracy of 0.0% and 0.08% and in the situation of moderate feedback $C/\alpha=3.000/4.000$, we obtained $\tilde{C}/\tilde{\alpha}=3.005/4.003$ with an accuracy of 0.17% and 0.08%, respectively. It should be noted that the accuracy is calculated by $\left|C-\tilde{C}\right|/C$ and $\left|\alpha-\tilde{\alpha}\right|/\alpha$. The estimation errors for above parameters are due to the error associated with the polynomial fitting of the displacement curve. Generally speaking, the higher the order of the polynomial is, the more accurate the estimation can be.
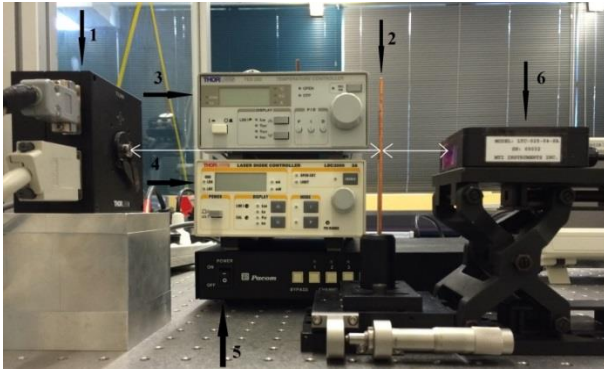
B.Experimental verification

Fig. 4. Experiment set-up including the SMI system and a commercial displacement sensor for verification; 1: Optical head including SL and PD, 2: External target, 3: Temperature controller, 4: SL controller, 5: Data acquisition circuit and 6: Commercial sensor LTC-025-04-SA for verification.

The proposed method has also been verified with the experimental data acquired using the set-ups shown as Fig. 4. The experimental set-ups include the SMI system and a commercial displacement sensor which is used to verify the movement of the target measured by the SMI. The commercial displacement sensor is LTC-025-04-SA from MTI instruments. For the SMI system, the optical head indicated by 1 in Fig. 4, contains the SL (HL8325G from HITACHI), a focusing lens and

a thermal resistance. In the experiment, the SL operated under the control of the SL controller LDC 2000 (indicated by 3) and the temperature controller TED 200 (indicated by 4) from the ThorLabs. The SL was biased at110 mA and operated in single longitudinal mode with an emitting wavelength of $0.8\,\mu m$. During the experiments, the operating temperature was kept at $23\pm0.1°C$. We employed a rectangle metal plate as the external target, marked as 2 in Fig. 4. Using this experimental set up, the SMI signal can be obtained for the target 20-600 mm away from the SL. In the following experiment, the target was placed at the distance of 310 mm (L_0) to the SL. The arbitrary movement was generated by applying a short impulse force on the metal plate. The SMI system and the commercial sensor (marked as 6) measured the movement trace of the target on the same position simultaneously but from the two opposite sides as shown in Fig. 4. Hence the movement trace measured by the SMI should be the inversed version of the result obtained from the commercial displacement sensor. The experiment results are depicted in Fig. (5). The Fig. 5 (a) shows the result from the sensor LTC-025-04-SA. For the convenience of the comparison, we also plotted the inversed version of Fig. 5(a) in Fig. 5(b). Fig. 5(c) is the measurement result obtained by the proposed method and Fig. 5(d) is the difference between measurement results obtained by the commercial sensor and the proposed method. The parameter estimation results related to the SMI, α and C, are 4.436 and 3.758, respectively. As can be seen from Fig. 5, the $\Delta L_{est}(t)$ in Fig. 5(c) is very close to the one, $\Delta L_{\mathrm{LTC-025-04-SA}}(t)$, shown in Fig. 5(b). The difference between $\Delta L_{est}(t)$ and $\Delta L_{\mathrm{LTC-025-04-SA}}(t)$ shows a maximum deviation of $0.294\,\mu m$. The relative large difference is due to the low resolution ($0.5\,\mu m$) of the commercial sensor.
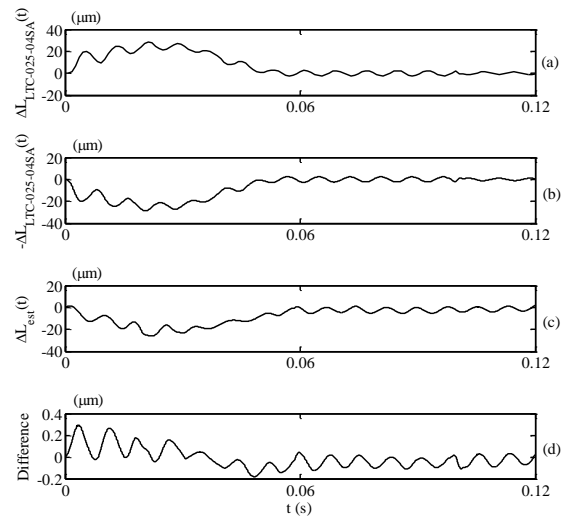

Fig. 5. Experimental verification result

4.Conclusion

For an SMI system with high resolution sensing, the measurement on the target movement requires the pre-

knowledge of the parameters associated with the SL, and inversely, the measurement on the SL related parameters requires knowing the waveform of the moving target. The proposed method in this paper solved the above problem by simultaneously measuring multiple parameters including the parameters associated with SLs and the arbitrary trajectory of the target. Unlike the method in [21] where the target is limited as a periodical movement, this paper considers a target with movement in arbitrary form and derives a new measurement matrix equation. Furthermore, to improve the measurement accuracy, all the available data samples obtained from an SMI system are employed in building the matrix equations and the total least square approach is used to estimate the multiple parameters. Implementation of the proposed method is presented in the paper. Simulations and experiments are conducted to verify the proposed method.

Reference

[1] S. Donati, M. Norgia, and G. Giuliani, "A review of self-mixing techniques for sensing applications," in *Optoelectronic and Microelectronic Materials and Devices*, 2004, pp. 260-261.

[2] Y. Yu, G. Giuliani, and S. Donati, "Measurement of the linewidth enhancement factor of semiconductor lasers based on the optical feedback self-mixing effect," *Photonics Technology Letters, IEEE,* vol. 16, pp. 990-992, 2004.

[3] C. Bes, G. Plantier, and T. Bosch, "Displacement measurements using a self-mixing laser diode under moderate feedback," *Instrumentation and Measurement, IEEE Transactions on,* vol. 55, pp. 1101-1105, 2006.

[4] Y. Yu, C. Guo, and H. Ye, "Vibration Menasurement Based on Moderate Optical Feedback Self-Mixing Interference [J]," *Acta optica sinica,* vol. 8, p. 018, 2007.

[5] Y. Yu, J. Xi, J. Chicharo, and T. Bosch, "Toward Automatic Measurement of the Linewidth-Enhancement Factor Using Optical Feedback Self-Mixing Interferometry With Weak Optical Feedback," *Quantum Electronics, IEEE Journal of,* vol. 43, pp. 527-534, 2007.

[6] D. Guo, M. Wang, and S. Tan, "Self-mixing interferometer based on sinusoidal phase modulating technique," *Optics Express,* vol. 13, pp. 1537-1543, 2005/03/07 2005.

[7] J. Xi, Y. Yu, J. Chicharo, and T. Bosch, "Estimating the parameters of semiconductor lasers based on weak optical feedback self-mixing interferometry," *Quantum Electronics, IEEE Journal of,* vol. 41, pp. 1058-1064, 2005.

[8] Y. Yu, X. Qiang, Z. Wei, and X. Sun, "Differential displacement measurement system using laser self-mixing interference effect," *Acta Optica Sinica,* vol. 19, pp. 1269-1273, 1999.

[9] L. Wei, X. Jiangtao, Y. Yanguang, and C. Joe, "Linewidth enhancement factor measurement based on optical feedback self-mixing effect: a genetic algorithm approach," *Journal of Optics A: Pure and Applied Optics,* vol. 11, p. 045505, 2009.

[10] Y. Fan, Y. Yu, J. Xi, and J. Chicharo, "Improving the measurement performance for a self-mixing interferometry-based displacement sensing system," *Appl. Opt.,* vol. 50, pp. 5064-5072, 2011.

[11] Y. Yu, J. Xi, and J. Chicharo, "Measuring the feedback parameter of a semiconductor laser with external optical feedback," *Opt. Express,* vol. 19, pp. 9582-9593, 2011.

[12] S. Donati, "Developing self-mixing interferometry for instrumentation and measurements," *Laser & Photonics Reviews,* vol. 6, pp. 393-417, 2012.

[13] S. Donati, G. Giuliani, and S. Merlo, "Laser diode feedback interferometer for measurement of displacements without ambiguity," *Quantum Electronics, IEEE Journal of,* vol. 31, pp. 113-119, 1995.

[14] N. Servagent, F. Gouaux, and T. Bosch, "Measurements of displacement using the self-mixing interference in a laser diode," *Journal of Optics,* vol. 29, p. 168, 1998.

[15] G. Giuliani, S. Bozzi-Pietra, and S. Donati, "Self-mixing laser diode vibrometer," *Measurement Science and Technology,* vol. 14, p. 24, 2003.

[16] A. Magnani, A. Pesatori, and M. Norgia, "Self-mixing vibrometer with real-time digital signal elaboration," *Applied Optics,* vol. 51, pp. 5318-5325, 2012/07/20 2012.

[17] O. D. Bernal, U. Zabit, and T. Bosch, "Study of Laser Feedback Phase Under Self-Mixing Leading to Improved Phase Unwrapping for Vibration Sensing," *Sensors Journal, IEEE,* vol. 13, pp. 4962-4971, 2013.

[18] A. Doncescu, C. Bes, and T. Bosch, "Displacement Estimation with an Optical Feedback Interferometer using an Evolutionary Algorithm," in *Sensors, 2007 IEEE*, 2007, pp. 382-386.

[19] M. Wang and G. Lai, "Displacement measurement based on Fourier transform method with external laser cavity modulation," *Review of Scientific Instruments,* vol. 72, pp. 3440-3445, 2001.

[20] J. Perchoux, L. Campagnolo, L. Yah Leng, and A. D. Rakic, "'Lens-free' self-mixing sensor for velocity and vibrations measurements," in *Optoelectronic and Microelectronic Materials and Devices (COMMAD), 2010 Conference on*, 2010, pp. 43-44.

[21] Y. Yu, J. Xi, J. F. Chicharo, and T. M. Bosch, "Optical Feedback Self-Mixing Interferometry With a Large Feedback Factor : Behavior Studies," *Quantum Electronics, IEEE Journal of,* vol. 45, pp. 840-848, 2009.

[22] J. Xi, Y. Yu, E. Li, and J. F. Chicharo, "An improved dynamic model for optical feedback self-mixing interferometry-based measurement and instrumentation," in *Signal Processing and Its Applications, 2005. Proceedings of the Eighth International Symposium on*, 2005, pp. 871-874.

[23] R. Lang and K. Kobayashi, "External optical feedback effects on semiconductor injection laser properties," *Quantum Electronics, IEEE Journal of,* vol. 16, pp. 347-355, 1980.

[24] Y. Yu and J. Xi, "Influence of external optical feedback on the alpha factor of semiconductor lasers," *Opt. Lett.,* vol. 38, pp. 1781-1783, 2013.

[25] M. Osinski and J. Buus, "Linewidth broadening factor in semiconductor lasers--An overview," *Quantum Electronics, IEEE Journal of,* vol. 23, pp. 9-29, 1987.

[26] T. Fordell and A. M. Lindberg, "Experiments on the Linewidth-Enhancement Factor of a Vertical-Cavity Surface-Emitting Laser," *Quantum Electronics, IEEE Journal of,* vol. 43, pp. 6-15, 2007.

[27] L. Wei, J. Chicharo, Y. Yu, and J. Xi, "Pre-Processing of Signals Observed from Laser Diode Self-mixing Intereferometries using Neural Networks," in *IEEE*

International Symposium on Intelligent Signal Processing, 2007. WISP 2007. , 2007, pp. 1-5.

[28] Y. Yu, J. Xi, and J. Chicharo, "Improving the Performance in an Optical feedback Self-mixing Interferometry System using Digital Signal Pre-processing," in *IEEE International Symposium on Intelligent Signal Processing, 2007. WISP 2007.* , 2007, pp. 1-6.

[29] Y. Gao, Y. Yu, J. Xi, and Q. Guo, "Simultaneous measurement of vibration and parameters of a semiconductor laser using self-mixing interferometry," *Applied Optics,* vol. 53, pp. 4256-4263, 2014/07/01 2014.

[30] S. Van Huffel and J. Vandewalle, *The total least squares problem: computational aspects and analysis* vol. 9: Siam, 1991.

[31] G. H. Golub and C. F. Van Loan, "An analysis of the total least squares problem," *SIAM Journal on Numerical Analysis,* vol. 17, pp. 883-893, 1980.